

# Strengthening of plasma treated 3D printed ABS through epoxy infiltration

Rafael J. Zaldivar<sup>1</sup> · Tait D. McLouth<sup>1</sup> · Dhruv N. Patel<sup>1</sup> · Joseph V. Severino<sup>1</sup> · Hyun I. Kim<sup>1</sup>

Received: 9 May 2017 / Accepted: 2 August 2017 / Published online: 31 August 2017  
© Springer International Publishing AG 2017

**Abstract** 3D printed fused deposition modeling (FDM) material parts have distinct anisotropic mechanical properties based upon their as-built print orientation. The strength of material printed perpendicular to the deposition layers can be as low as 50% of values for injection molded parts due to less than optimum interlayer fusion, limiting their use for critical applications. The focus of this work is to present a novel way of utilizing design freedoms available in FDM to improve strength in weak orientations. Vertically processed FDM ABS parts were manufactured with cavities printed perpendicular to the interlayer direction and were subsequently plasma surface treated, filled with an epoxy resin, and mechanically tested. Plasma treatment was shown to beneficially modify the surface chemistry, which resulted in a 50% improvement in shear strength over untreated specimens. Samples that underwent plasma treatment and epoxy infiltration demonstrated a 130% increase in flexural strength over that of as-printed FDM material. The failure strain was also shown to increase by two-fold. The addition of milled carbon fiber (MCF) filler within the epoxy infiltrate was also evaluated and was shown to increase the flexural modulus by as much as 76% at 10 wt% loading levels, though negligible increases in strength were observed.

**Keywords** Additive manufacturing · FDM · Plasma treatment · Mechanical properties · ABS

## 1 Introduction

Additive manufacturing (AM) of polymers continues to advance as a promising technology due to the potential to more easily process complex parts and increase manufacturing productivity [1, 2]. One process that has been extensively utilized in the manufacturing of polymeric 3D printed parts is Fused Deposition Modeling (FDM). FDM is an additive manufacturing process based on a computer-aided design (CAD) where a thermoplastic polymer is extruded through a heated nozzle and deposited, layer-by-layer, in a sequential process to build a part. Several researchers have shown that the inherent nature of the FDM process leads to less than ideal consolidation of layers [3, 4]. Tensile properties of FDM processed ABS alone have been reported to range from 11 to 40 MPa and the compressive properties of the same material can vary from 30 to 40 MPa based on print orientation [3, 5, 6]. This variation in mechanical performance is a result of the anisotropic nature of these parts along with added contributions related to the number of significant processing variables available (e.g. layer thickness, raster pattern, extrusion temperature, etc.) within the FDM process. Torrado-Perez et al. [7] and Hambali et al. [8] have shown that the average tensile strength decreases as a function of print orientation relative to the load direction for a number of AM resin systems (ABS, PLA, Nylon, and polycarbonate). Recently, Zaldivar et al. showed a similar behavior using ULTEM parts processed in the vertical build direction which resulted in strength utilization values of only 46% that of conventionally processed injection molded ULTEM [9].

Although FDM structures have the potential to replace an ever-increasing number of parts used in space hardware, their limitations due to build print orientation effects may

✉ Rafael J. Zaldivar  
Rafael.j.zaldivar@aero.org

<sup>1</sup> The Aerospace Corporation, El Segundo, USA, California

constrain their use to non-structural applications. Previous work by Belter and Dollar have successfully implemented a method that provides an additional margin in the strength and stiffness of FDM processed 3D parts [10]. They have shown that by infiltrating open or sparsely filled voids with high strength resins, significant improvements in mechanical properties can be achieved. The infiltration of resin within these areas provides a more efficient stitching of weak plane directions as well as replaces an anisotropic material with a higher strength isotropic epoxy. However, numerous studies have shown that adhesives do not typically bond well to thermoplastics resins used in 3D printing, reducing their ability to transfer stress and achieve strong bonds for efficient utilization [11, 12].

Plasma treatment has been shown to improve bonding in a number of polymer systems as well as a few structural composites materials systems with promising results [13, 14]. The plasma can activate a species such as oxygen gas forming a highly reactive atomic oxygen free radical. This highly reactive species can then interact with the outermost nanometers of the treated surface forming chemically bonded polar groups such as carboxyl, carbonyl, and hydroxyl moieties [15]. In some cases, these chemical groups on the substrate have been shown to further react with the adhesive used for bonding to form strong chemically bonded interfaces. In addition, plasma treatment has been shown to effectively remove low molecular weight hydrocarbon contaminants as well as promote localized etching of the material which may also contribute to improvements in interfacial bonding.

Vacuum plasma treatment was selected for this experiment as it allows for the treatment of internal channels in complex FDM parts. As shown in Fig. 1, samples can be placed inside of a vacuum plasma chamber, which is then

filled with gas at a low pressure [16]. The gas is energized by a radio frequency (RF) giving rise to the interactions between plasma ions and the exposed surfaces of the sample being treated [17].

In this report, we investigate the effect of vacuum plasma treatment on the wetting characteristics, surface chemistry, and shear strength of epoxy infiltrated FDM processed ABS parts. We then evaluate whether the effect of these processes can further improve the flexural strength of vertically manufactured FDM parts. Finally, the effect of carbon fiber filler concentration on the mechanical performance of the infiltrated system will also be evaluated.

## 2 Experimental

### 2.1 Materials

All parts were manufactured using a Stratasys 3D production system (Fortus 250 mc, Eden Prairie, MN, USA). The accompanying software, Insight (Version 10.2, Eden Prairie, MN, USA), was used to control the process of fabricating parts with the 250 mc loaded using a Stereo lithography (STL) file. Acrylonitrile butadiene styrene copolymer (ABS) was the material of choice for all builds investigated in this study. The T16 tip, which produces a 0.178 mm slice height was used in this study. The build density, raster width, raster-starting angle, and raster delta angle air gap were optimized based on the software input data. Predetermined channels through the FDM specimens were infiltrated with a West System 105/205 epoxy resin/hardener system. The epoxy mixture was mixed using a FlackTek planetary mixing system (Model DAC 150.1 FVZ-K, Landrum, SC, USA) at 3000 rpm for 3 min. The samples were cured for 4 days at room temperature. The filled system utilized Zoltek PX35 milled carbon fiber. The fiber has a diameter of 7.2  $\mu\text{m}$  with an average fiber length of 100  $\mu\text{m}$ . The loading concentrations investigated in this study were 1, 2, 5, and 10 wt%.

### 2.2 Vacuum plasma treatment

Plasma treatment of the 3D printed ABS material was performed using an AutoGlow Plasma treatment chamber (Model 200, Tempe, AZ, USA). Specimens were 3D printed into 3.8 cm (outer diameter) annular specimens with an inner radius of 1.2 cm. Each of these specimens was placed in the plasma treatment oven and treated at 13.56 MHz. The specimens were placed under vacuum and the oxygen active gas was flowed in at a rate of 2.5 cc/min. The power was then initiated to start the plasma and held for various durations (0, 1, 2, and 5 min) to optimize the surface treatment condition of the ABS material. The

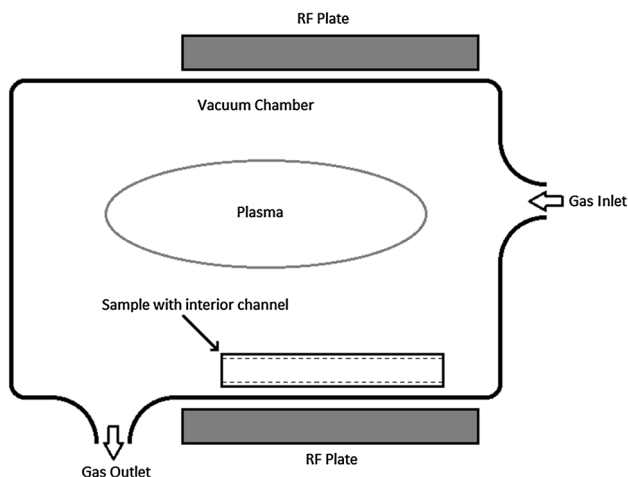


**Fig. 1** Schematic of a vacuum plasma system, with a sample shown inside

infiltrate was then poured into the center annulus within 1 h of treatment.

### 2.3 Contact angle measurements

A Rame-Hart Advanced Automated Digital Goniometer (Model 260-F4, Succasuna, NJ, USA) was used for all contact angle measurements. The test unit utilizes DROPImage Advanced software (Version 2.6.1, Succasuna, NJ, USA) for resolving all contact angle measurements and surface energy analysis on  $25 \times 25$  mm printed ABS specimens. The specimens were cleaned using isopropanol, and plasma treated at various durations of treatment time (0, 1, 2, and 5 min) to evaluate the effect on the wetting angle.

### 2.4 X-ray photoelectron spectroscopy

A physical electronics X-ray Photoelectron spectroscopy (XPS) system (VersaProbe II, Chanhassen, MN, USA) using Al K $\alpha$  source was used for surface chemical analysis as a function of plasma treatment of the FDM processed ABS specimens. Analyzer pass energies of 187.85 and 46.95 eV were used for wide scans and high-resolution spectra, respectively. The XPS analysis chamber was pumped by an ion pump and had a base pressure of  $1 \times 10^{-10}$  Torr.

### 2.5 Mechanical testing

Beam samples were printed with a sample geometry of  $12.7 \times 1.27 \times 0.635$  cm. The 3-point bend support span was approximately 10.16 cm and testing was in accordance with ASTM D790 [18]. The testing was performed using a 5kN load cell and a crosshead speed of 0.254 cm/min. Interfacial shear strength testing was performed on the aforementioned annular ring specimens before and after plasma treatment. These tests were performed under a ram compressive load using an Instron universal testing machine (Model 5500, Norwood, MA, USA). A 250kN-load cell was used and the testing was performed at 0.254 cm/min.

## 3 Results and discussion

The strength of FDM manufactured hardware is believed to be a function of numerous factors: the inherent bulk polymer strength, the geometry and degree of porosity, the extent of fiber-to-fiber fusion, and the layer orientation relative to the load direction. While each of these factors contributes to differing degrees, the build print orientation with respect to the load direction has been shown to be the

most critical in determining final mechanical properties [9]. Figure 2 shows a schematic of the various part mesostructures observed for each of the build designations. Dashed lines represent raster patterns and solid lines represent the layers within the part. The primary axial load direction is shown with arrows in the schematic. This is the direction by which the load is applied to the surface of the tensile face of the flexural specimen. Both the specimens processed on edge and in the flat configuration result in layers oriented axially along the test load direction. On the other hand, specimens that were fabricated in the vertical configuration result in layers perpendicular to the load direction. Figure 3 shows examples of the flexural stress strain curves for the FDM processed beams manufactured in the different build configurations and tested in the axial direction shown in Fig. 2.

As shown, the samples fabricated in the flat and edge direction yield similar mechanical properties, while fabrication in the vertical direction results in a part with significantly lower failure strength and failure strain values. The vertical processed specimens have flexural strengths approximately 35% of edge processed specimens and failure strains as much as 78% lower than the other two configurations. These degraded mechanical property results are primarily due to delaminations occurring at the weaker layer-to-layer interfaces in the vertically built specimen. On the other hand, the build print orientation appears to have little effect on the flexural modulus as shown in Fig. 3. Table 1 summarizes the mechanical properties values for all three print orientations.

To overcome these weak layer-to-layer deficiencies, segments of the anisotropic FDM specimen were replaced with an isotropic epoxy. In other words, inner segments were printed out as channels and then infiltrated with an epoxy resin. However, prior to infiltration, studies were performed to determine a surface preparation methodology to optimize the bond strength and wetting behavior between the epoxy infiltrate and the FDM processed ABS.

Both vacuum and atmospheric plasma treatment have been shown to enhance the wetting behavior of polymers by forming more polar groups on the surface [19]. Flat ABS specimens were printed and plasma treated for

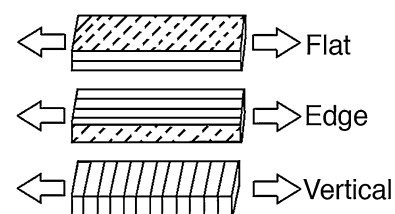


**Fig. 2** Schematic showing raster patterns and layer orientation for several print orientations. (dotted lines raster pattern, solid lines build layers)

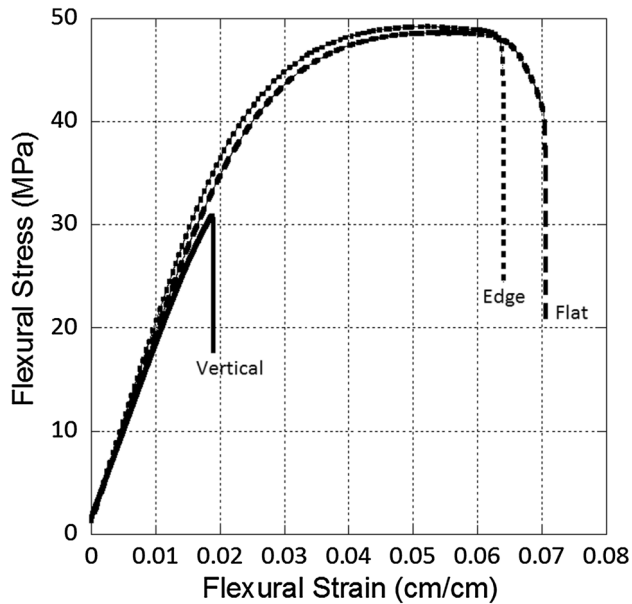


**Fig. 3** Stress-strain profile for ABS printed in several configurations (vertical, edge, flat)

**Table 1** Summary of mechanical properties of FDM processed ABS

Sample	Flexural strength (MPa) (%)	Flexural modulus (GPa) (%)	Failure strain (cm/cm) (%)
Flat	47.7 ± 1.6	1.77 ± 1.6	0.07 ± 4.6
Edge	49.1 ± 0.4	1.94 ± 0.2	0.07 ± 3.0
Vertical	31.1 ± 0.6	1.73 ± 1.4	0.02 ± 0.9

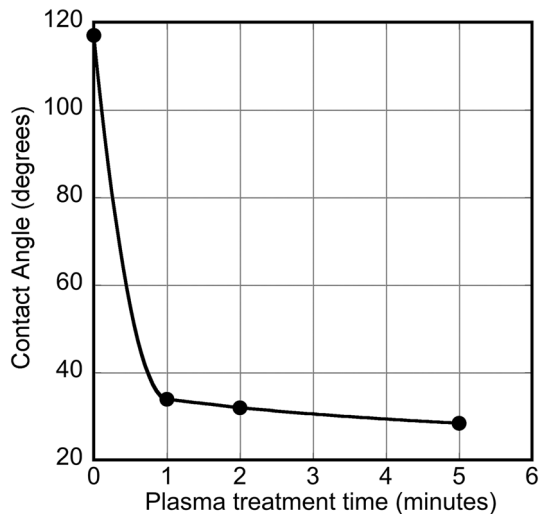


**Fig. 4** Contact angle measurements as a function of plasma treatment duration for FDM ABS

various durations and their wettability was measured by contact angle analysis. Figure 4 shows the wetting characteristics of the FDM ABS as a function of treatment time.

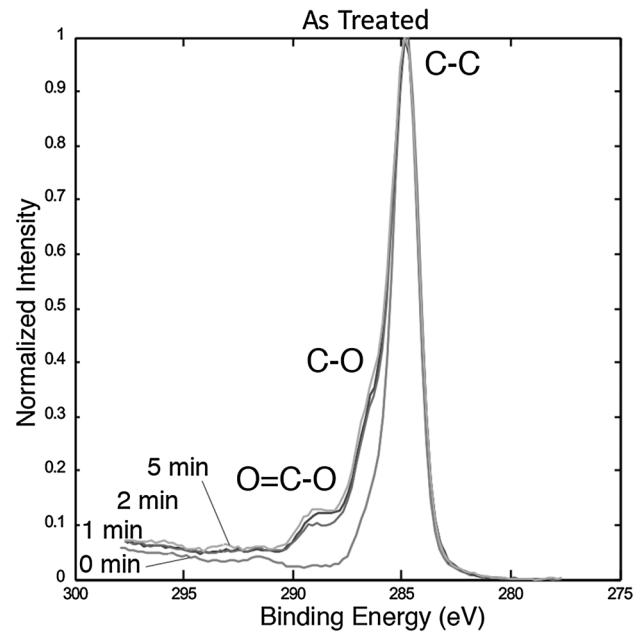


**Fig. 5** High-resolution spectra of the functional groups formed with plasma treatment on the surface of the ABS material

Initially the contact angle is approximately 118 degrees, indicating extremely poor wettability; however, after only 1 min of plasma treatment, the contact angle is observed to decrease significantly to 32 degrees. Further plasma treatment shows a more gradual decrease in contact angle as seen in Fig. 4, which is typical once saturation has occurred. Changes to the wetting characteristics of the substrate of this magnitude are very promising and are expected to improve infiltration of the epoxy. However, wetting alone does not ensure improved bonding at the ABS substrate to adhesive interface. The specific type of functional group formed with treatment has been shown to more directly correlate with increases in bond strength [15].

XPS was performed to analyze what surface chemical modifications were induced to the substrate surface as a function of plasma treatment. Figure 5 shows an example of the high-resolution spectra for the ABS material as a function of treatment time. As shown, oxygen functional groups are formed after only 1 min of treatment which correlates with the improvement observed in wetting characteristics shown in Fig. 4. A detailed analysis of the XPS spectra of the C 1s region shown in Fig. 5 allows a closer examination of the specific functional groups contributing to improvements in wetting. The singular peak at 284.6 eV can be attributed to C–C and C–H bonds in the polymer backbone, and it is the most dominating species before any plasma exposure. Subsequent exposure of the surface creates new peaks at the shoulder of the main peak on the higher binding energy side, related to binding energies for the new functional groups created at 286.3 and

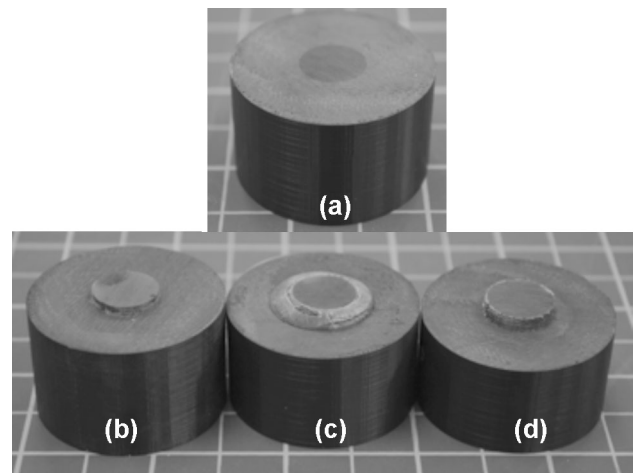
288.8 eV. The peak at 286.3 eV is attributed to alkoxy groups (C–O) while the peak at 288.8 eV is representative of carboxyl groups (O–C=O). Both are polar functional groups that can interact with reactive groups in the infiltrating epoxy. Further plasma treatment exposure shows only slight changes in the concentration of functional groups formed as shown in Table 2. This again corresponds to the relative changes observed using contact angle analysis.

Table 2 shows the total oxygen content with respect to carbon ratio for ABS as a function of treatment time, for both as-treated and solvent rinsed ABS. As duration exposure increases, an increase in surface oxygen levels is also observed. These results agree with previous studies [11–15]. However, previous investigations have also shown that the as-treated oxygen levels may not necessarily represent the functional groups participating in the chemical bonding between the treated surface and the epoxy infiltrate. We have observed that there are small fragments of the polymer that have been detached from the backbone structure due to excess oxidation [19]. This non-adhered material or ash, although highly functionalized, would not contribute to improvements in mechanical performance. A rinse of the plasma treated substrate using a polar solvent such as isopropyl alcohol (IPA) allows one to better evaluate if excessive degradation or damage of the surface has occurred. A relatively large variation between the O/C ratio of the as-treated surface to the same surface after a solvent rinse provides an indication as to the level of degradation or loosely bound ash that has been generated. Table 2 shows that O/C levels for the various plasma treatment durations before and after solvent rinse do not vary significantly, even beyond the saturation point at 1 min.

To evaluate the effect of plasma treatment on interfacial shear strength between the epoxy and the FDM ABS part, a number of annular ABS specimens were printed and

**Table 2** Vacuum plasma treatment of FDM ABS pre- and post-solvent rinse

Minutes	O/C	C–C	C–O	O–C=O
As-treated (before rinse)				
0	0.09	92.1	7.1	0.0
1	0.32	72.6	21.0	6.4
2	0.30	74.5	21.0	4.5
5	0.33	71.3	22.2	6.6
After rinse				
0	0.09	92.1	7.1	0.0
1	0.27	76.9	19.2	4.0
2	0.25	77.2	18.5	4.3
5	0.29	73.8	22.0	4.2



**Fig. 6** Test specimen and failure mode for various plasma treatment times (a) pre-test (b) control (untreated) post-test (c) 2-min plasma post-test (d) 5-min plasma post-test

infiltrated with epoxy in the center. The ABS was plasma treated for various durations prior to infiltration and cure. Figure 6a shows a photograph of the test specimen prior to testing. Samples were tested by applying a compressive load to the center portion (cured epoxy) of the part, resulting in a shear failure at the interface between the cured epoxy and the ABS printed part. Figure 7 shows examples of the shear stress with displacement curves for these specimens. The control, untreated sample reached a peak stress of approximately 13.1 MPa ± 8%, and then failed at this peak load. Figure 6b shows the interfacial fracture surface of the untreated specimen after failure. The inner epoxy cylinder is shown protruding cleanly from the surrounding ABS material. For the 1-min plasma treated sample, the peak shear stress increases from the untreated

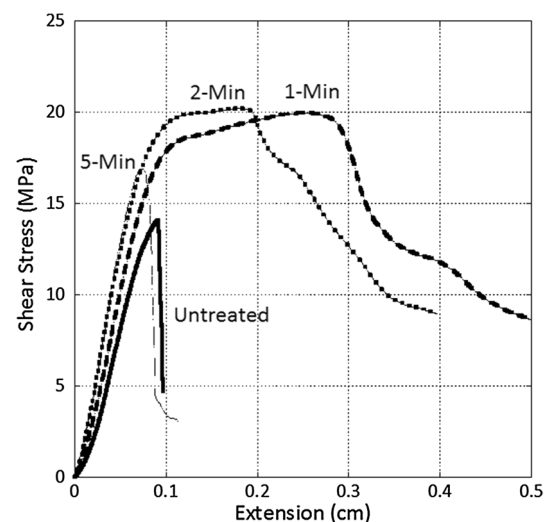


**Fig. 7** The effect of plasma treatment duration on shear strength of epoxy infiltrated FDM ABS parts

value by 50% to  $20.0 \text{ MPa} \pm 2\%$ . The shear stress displacement curve also appears to maintain load over a larger displacement range ( $3\times$  un-treated displacement) indicating a stronger and more resilient bond has formed after treatment. Further plasma treatment up to 2 min results in a similar peak shear strength value of  $20.0 \text{ MPa} \pm 2\%$ . However, the peak stress level drops off after a slightly reduced displacement level. Figure 6c shows a significant change in failure mode, consistent with the failure mode observed for the 1 min treated specimen. In both of these cases, the bond strength appears to have increased significantly at the ABS-to-epoxy interface, resulting in an ultimate failure occurring within the ABS material. Plasma treatment for 5-min prior to infiltration reduces the peak strength and failure strain with respect to the two prior plasma treatment conditions. However, the specimen still maintains a 25% increase over the untreated specimen at approximately  $17.2 \text{ MPa} \pm 8\%$  after treatment. It should be noted that the stress–deflection curve shown in Fig. 7 is more similar in nature to the untreated ABS material. On closer examination of the interface, the failure is not as clean as the untreated specimen, but rather shows a thin single layer of the ABS material bonded to the epoxy. We believe that this localized failure within the ABS may be due to excessive treatment in terms of thermal exposure inside the plasma chamber. No indications of excessive chemical oxidation were evident from our XPS solvent rinse tests described in Table 2.

After determining the optimum plasma treatment condition (1 min) for improved bonding, the effect of epoxy infiltration and surface treatment on the flexural properties of vertically processed ABS parts was evaluated. Figure 8 shows the representative flexural stress–strain curves for a 3D printed solid ABS beam processed in the vertical orientation compared to a similar sized specimen infiltrated with epoxy, with and without surface treatment. The as-is ABS specimens have poor flexural properties as shown from the plot. The breaking stress is approximately 30 MPa with a flexural modulus of 1.72 GPa. The infiltrated material dramatically increases the strength of the part by a value approximately 100% greater to 60 MPa. This improvement is achieved without any surface treatment. The specimens that are surface treated for 1 min prior to infiltration show an increase of over 121% in flexural strength over the base vertical printed ABS parts. In addition, the failure strain increases by over 1.3 times the value for the control ABS printed specimen. Changes in modulus increased from 1.72 to 2.26 GPa and 2.31 MPa for the untreated infiltrated specimens, and the 1 min plasma treated infiltrated specimens, respectively.

The effect of adding milled carbon fibers (MCF) into the epoxy infiltrate was also evaluated as a method to further modify mechanical properties of the part. Figure 9 shows

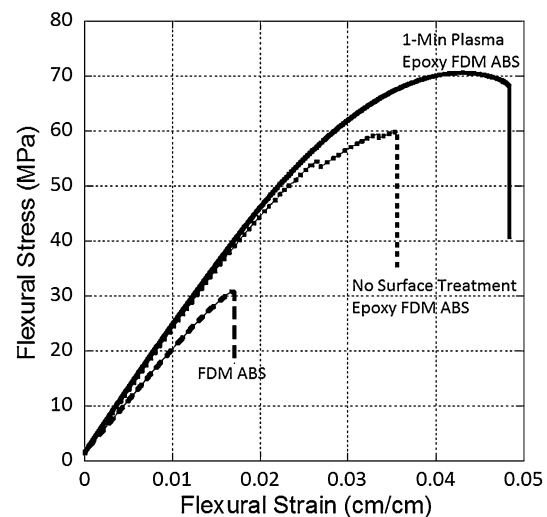


**Fig. 8** Effect of epoxy infiltrate in FDM processed ABS part with and without plasma treatment

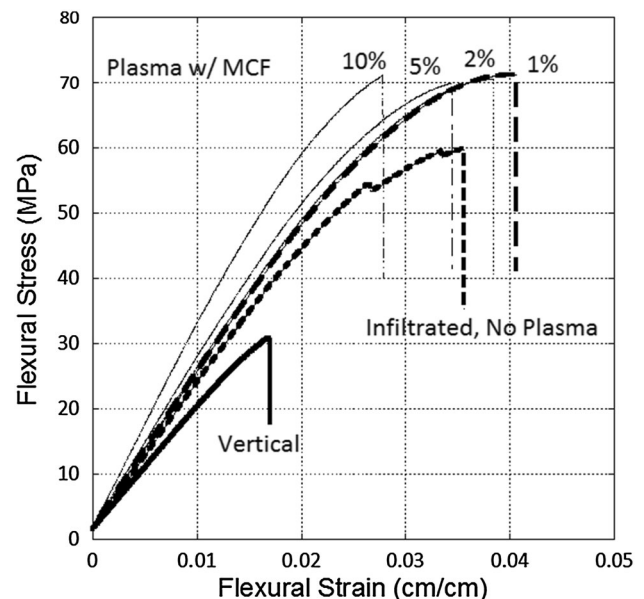


**Fig. 9** Flexural stress strain behavior as a function of process conditions. (a) as-printed (b) infiltrated, no surface treatment (c) infiltrated, 1-min surface treatment, 1% MCF (d) infiltrated, 1-min surface treatment, 2% MCF (e) infiltrated, 1-min surface treatment, 5% MCF (f) infiltrated, 1-min surface treatment, 10% MCF

the flexural stress–strain profile for the epoxy infiltrated ABS material as a function of loading condition. As previously described, there is a significant increase in breaking strength by incorporating the surface treated epoxy infiltrate method. Increasing the concentration of MCF from 1 to 10% shows little variation in the breaking strength. However, the strain-to-failure shows a consistent decrease with the amount of added MCF. Figure 10 shows the cross-sections of epoxy infiltrate with varying levels of carbon

**Fig. 10** Micrograph showing distribution and loading concentration of MCF in epoxy infiltrate (MCF white particles, voids black circles)

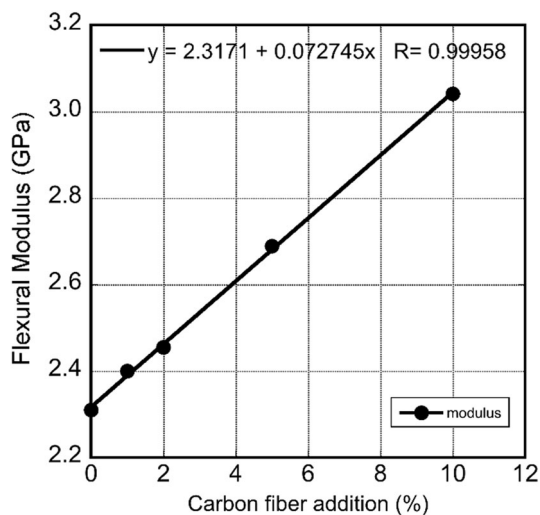
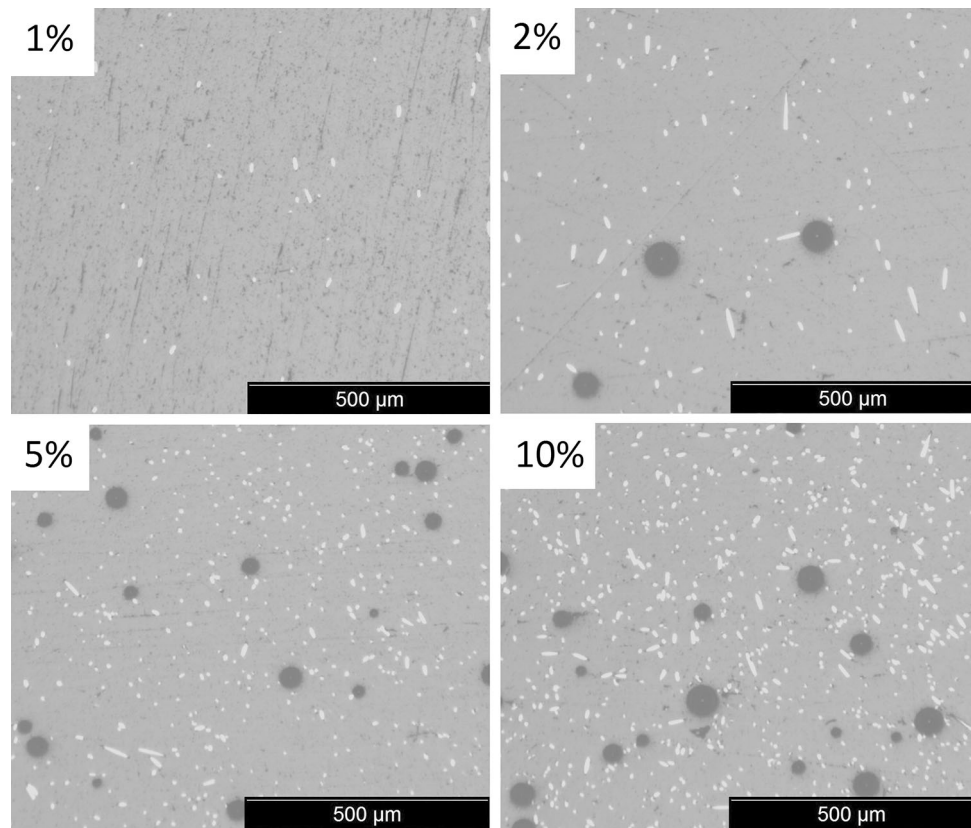


**Fig. 11** The Effect of carbon filler addition on the flexural modulus of the epoxy infiltrated specimens

filler addition. As shown, the samples appear to have good filler distribution for load concentrations ranging from 1 to 10% by weight. However, as the loading condition increases, there is a corresponding increase in the viscosity of the resin which was shown to increase the degree of observed porosity. This may be a contributor to the reduced failure strain.

In addition, as shown from the stress–strain curves shown in Fig. 9, a steeper slope with higher loading concentration indicates an increase in modulus. Figure 11 summarizes the changes in the flexural modulus as a function of filler concentration. The unfilled material yields a modulus of 2.3 GPa while the 10% loaded specimen has a greater than 35% increase in modulus to approximately 3.1 GPa. A summary describing the observed changes in mechanical properties for these modified FDM ABS parts is shown in Table 3.

#### 4 Conclusion

3D printed fused deposition modeling (FDM) material parts have distinct anisotropic mechanical properties based upon their as-built print orientation. The strength of the material printed vertically or perpendicularly to the deposition layers tends to be significantly weaker than other directions due to less than optimum interlayer fusion. Epoxy infiltration of a pre-determined void volume perpendicular to the build layer direction has been shown to significantly increase the flexural strength and failure strain of parts by overcoming weak interlayer bonding. The flexural strength increased by 90% from the as-printed condition through epoxy infiltration alone. Plasma

**Table 3** Effect of filler load concentration on mechanical performance

Sample	Flexural strength (MPa) (%)	Strength increase (%)	Flexural modulus (GPa) (%)	Modulus increase (%)	Failure strain (cm/cm) (%)
As-Printed	31.10 ± 0.6	N/A	1.73 ± 1.4	N/A	0.019 ± 0.9
Baseline	60.19 ± 3.2	93.63	2.26 ± 0.5	30.84	0.042 ± 34.4
1 min	68.74 ± 2.5	120.97	2.31 ± 2.7	33.67	0.044 ± 8.2
1%P	70.19 ± 1.3	125.70	2.40 ± 0.4	39.02	0.040 ± 3.8
2%P	70.53 ± 1.9	126.81	2.46 ± 0.3	42.15	0.042 ± 8.8
5%P	70.05 ± 1.1	125.34	2.69 ± 2.5	55.65	0.034 ± 5.5
10%P	68.74 ± 6.3	121.03	3.05 ± 2.2	76.16	0.027 ± 12.2

treatment improved wettability and shear strength by promoting chemical bonding between the FDM processed ABS and the infiltrated epoxy. Oxygen containing functional groups were observed to maximize on the surface of the material after only 1 min of treatment. Increases of over 50% in shear strength were observed after 1 min of plasma treatment. The combined effects of plasma treatment and epoxy infiltration resulted in an over 120% increase in both flexural strength and strain over the as printed condition. The addition of milled carbon fiber filler to the infiltrate was shown to have negligible increases in flexural strength but yielded as high as a 40% increase in stiffness over the unfilled epoxy. Epoxy infiltration combined with vacuum plasma treatment is an efficient way of improving mechanical properties of 3D printed structures in inherently weak print orientations.

#### Compliance with ethical standards

**Conflict of interest** On behalf of all author, the corresponding author states there is no conflict of interest.

#### References

1. Bagsik A, Schöppner V, Klemp E (2010) part quality manufactured with Ultem©9085. In: Proceedings of Inter Conf Polym Mater. Halle pp 1–8
2. Zhang Y, Chou K (2008) A parametric study of part distortions in fused deposition modeling using three-dimensional finite element analysis. *Proc Inst Mech Eng B* 222(8):959–968
3. Ahn SH, Montero M, Odell D, Roundy S, Wright PK (2002) Anisotropic material properties of fused deposition modeling ABS. *Rapid Prototyp J* 8:248–257
4. Bellehumeur C, Li L, Sun Q, Gu P (2004) Modeling of bond formation between polymer filaments in the fused deposition modeling process. *J Mater Process Technol* 6:170–178
5. Croccolo D, De Agostinis M, Olmi G (2013) Experimental characterization and analytical modelling of the mechanical behavior of fused deposition processed parts made of ABS-M30. *Compos Mater Sci* 79:506–518
6. Porter D, Hoang TV, Berfield TA (2017) Effects of in situ poling and process parameters on fused filament fabrication printed PVDF sheet mechanical and electrical properties. *Addit Manuf* 13:81–92
7. Torrado AR, Roberson DA (2016) Failure analysis and anisotropy evaluation of 3D-printed tensile test specimens of different geometries and print raster patterns. *J Fail Anal Preven* 16(1):154–164
8. Hambali RH, Celik K, Smith P, Rennie A, Ucar M (2010) Effect of build orientation on FDM parts: a case study for validation of deformation behaviour by FEA. In: *Inter. Conf. on Design and Concurrent Eng. (iDECON 2010): manufacturing challenges towards global sustainability*. Penerbit Universiti (UTeM). pp 224–228
9. Zaldivar RJ, Witkin D, McIlouth T, Patel D, Schmitt K, Nokes JP (2017) Influence of processing and orientation print effects on the mechanical and thermal behavior of 3D-printed ULTEM 9085 material. *Addit Manuf* 13:71–80
10. Belter JT, Dollar AM (2014) Strengthening of 3D printed robotic parts via fill compositing. In: *Inter. Conf. on Intelligent Robots and Systems (IROS)*. Chicago
11. Comyn J, Mascia L, Xiao G (1996) Plasma treatment of polyetheretherketone (PEEK) for adhesive bonding. *Intl J Adhes Adhes* 16(2):97–104
12. Abenojar J, Torregrosa-Coque R, Martinez M, Martin-Martinez J (2009) Surface modification of polycarbonate and acrylonitrile butadiene styrene (ABS) Copolymer by treatment with atomospheric plasma. *Surf Coat Technol* 203(16):2173–2180
13. Zaldivar RJ, Kim HI, Steckel G, Morgan B, Nokes JP (2011) Surface preparation for adhesive bonding of polycyanurate-based fiber-reinforced composites using atmospheric plasma treatment. *J Appl Polym Sc.* 120(2):921–931
14. Zaldivar RJ, Steckel GS, Morgan B, Kim HI (2012) Bonding optimization on Composite surfaces using atmospheric plasma treatment. *J Adhes Sci Technol* 26(1–3):381–401
15. Zaldivar RJ, Nokes J, Steckel G, Kim H, Morgan BA (2010) The effect of atmospheric plasma treatment on the chemistry, morphology and resultant bond behavior of a PAN-based carbon fiber reinforced epoxy composite. *J Compos Mater* 44(2):137–156
16. Shenton MJ, Stevens GC (2001) Surface modification of polymer surfaces: atmospheric plasma versus vacuum plasma treatments. *J Phys D Appl Phys* 34:2761–2768
17. Liston EM, Martinu L, Wertheimer MR (1994) Plasma surface modification of polymers for improved adhesion: a critical review. *Plasma Surf Modifi Polym* 489:3–39
18. ASTM D790 (2010) Standard test method for flexural properties of unreinforced and reinforced plastics and electrical insulating materials. *ASTM Intl, West Conshohocken*
19. Morgan B, Zaldivar RJ, Kim H, Steckel G, Chaney J, Nokes JP (2011) Effect of isopropanol rinse on the adhesion of plasma-treated Carbon-fiber reinforced composites. *J Compos Mater* 45(12):1331–1336